Journal of Statistical Physics, Vol. 34, Nos. 3/4, 1984

Order and Disorder Lines in Systems with Competing Interactions. III. Exact Results from Stochastic Crystal Growth

P. Ruján[1]

Received April 8, 1983; revised September 8, 1983

The methods presented in the first two articles of this series are simplified and generalized by growing stationary stochastic crystals from a given Ansatz layer. On the disorder trajectory the free energy, correlation functions, and multicritical points are calculated explicitly for a large class of models with competing interactions, including the staggered eight-vertex model, the general sixteen-vertex model, the q-state Potts model on a triangular lattice, a general $Z(q)$ model, and restricted spin glass models in two dimensions.

KEY WORDS: Disorder lines; exact results; q-state spin models.

1. INTRODUCTION

This is the last article in a series of papers devoted to the systematic study of order and disorder lines in systems with competing interactions. The order (disorder) lines are given trajectories of the parameter space lying on ordered (disordered) phases of the model. In these subspaces the competition between different ordering tendencies has a spectacular result in simplifying the correlation functions and sometimes making the model exactly soluble through an effective dimensionality reduction.

In the first article[1] (referred to henceforth as I) the Hamiltonian of spin-1/2 quantum chains had been interpreted as the time evolution (Liouville) operator of a kinetic Ising model[2] for a special choice of

[1] Institute for Theoretical Physics, Eötvös University, H-1088 Budapest, Puskin u. 5-7, Hungary.

0022-4715/84/0200-0615$03.50/0

coupling constants. In the second article[3] (referred to hereafter as II) the transfer matrix formalism had been used to calculate disorder trajectories and their duality generated analytic continuation (order lines) in a model with all possible interactions around a face of the square lattice (IRF model).

The disorder phenomena are not simply a mathematical curiosity but have a rich physical content (see I). They provide exact information on a remarkably large subspace of very complicated models, and they form a solid basis for further investigations. As an example, we note here the recent calculation of the generating function of directed animals in two and three dimensions.[4]

In this article a simple crystal growth model method, as first introduced by Enting[5] and Verhagen[6] in the context of Ising models, is related to the previously used methods. Although technically equivalent to the methods used in I and II, this new formulation proves to be more flexible in dealing with general (asymmetric) cases. Also, it is a more direct approach since one constructs the model from the Ansatz instead of searching for the Ansatz appropriate to a given model (as in II). This makes the calculations easier and more transparent. It turns out that the crystal growth models[7] correspond to a commonly used Monte Carlo algorithm. When searching for disorder lines one uses equilibrium crystals, exactly as in the Peschel and Emery method.[2,3]

It seems very interesting to consider also the problem of nonequilibrium crystals, but this problem is not treated here.

The paper is organized as follows. In Section 2 the crystal growth method is exposed and discussed in detail. The eight-vertex model is reconsidered in Section 3; it turns out that the model can be exactly solved in a four-dimensional subspace of its five-dimensional parameter space. The correlation functions are calculated and it is shown that within the four-dimensional disorder space there is a three-dimensional subspace where the correlation functions exhibit a purely one-dimensional, single exponential decay (see II). This means that it is possible to monitor a change from a monotonic to a modulated exponential decay within the disorder subspace itself. The general disorder subspace of the staggered eight-vertex model is treated in Section 4. Special cases leading to the Union Jack lattice, to the Ashkin–Teller, and to the ANNNI model are treated in detail. Section 5 contains the most complicated Ising-type model considered here, the staggered IRF model, which includes the sixteen-vertex model as a special case. The calculation of the free energy and correlation functions may be obtained numerically—formulas are provided to this end. The q-state Potts model with one- and two-body external fields on a triangular lattice is considered in Section 6. The model can be exactly

solved on a five-dimensional subspace of its seven-dimensional parameter space for arbitrary q values. Again, the free energy and the correlation functions are explicitly calculated.

Other q-state models, in particular general $Z(q)$ models on a triangular lattice, are considered in Section 7. If there are no external fields, remarkably simple formulas are obtained for the disorder constraint, the free energy, and the correlation functions. Finally, in Section 8 it is shown that the method applies as well when the competing interactions are also random variables. If a local disorder constraint is satisfied, the random anisotropic triangular Ising model is exactly soluble for arbitrary quenched distributions of bonds. Except for the randomly layered[8] free fermion models, this seems to be the only exact solution for a spin glass model in two dimensions.

Whenever possible the analytic continuation of the results is obtained through the duality transformation[3] and through the matrix inversion relation.[9] Because of the large number of models considered it seems appropriate to comment on the notation. Ansatz parameters are usually denoted by small Greek letters. Couplings appearing in the normalization factors are denoted by capital letters A, B, etc., while small letters a, b, . . . etc. denote intermediate expressions. The couplings of the resulting "crystal" model are denoted by the capital letters $K, L, \ldots$ (also H for external fields).

2. GROWING STOCHASTIC CRYSTALS

The crystal growth models are simple stochastic models where the crystal is supposed to grow layer after layer in a direction perpendicular to a given Miller plane.[5,7] The new layer of atoms is built up atom by atom following a given prescription (ordering). Each atom is "adsorbed" or rejected with a given probability conditional on the actual configuration of its predecessors [neighboring atoms on the previous layer(s)]. We shall not pursue further the details of crystal growth models. Instead, we would like to make the connection between this model of crystal growth and kinetic Ising models. In view of the methods presented in I and II the procedure to be followed here is quite transparent: one constructs a time evolution process leaving invariant the Boltzmann distribution of the (d-dimensional) Ansatz problem, thus defining a $(d+1)$-dimensional lattice model at a disorder line. This interpretation makes the method used by Verhagen[6] very simple, allowing for a straightforward generalization to q-state models and random spin models.

We now proceed to construct the first layer of the crystal—the Ansatz problem. As in II one may consider as an example a one-dimensional Ising

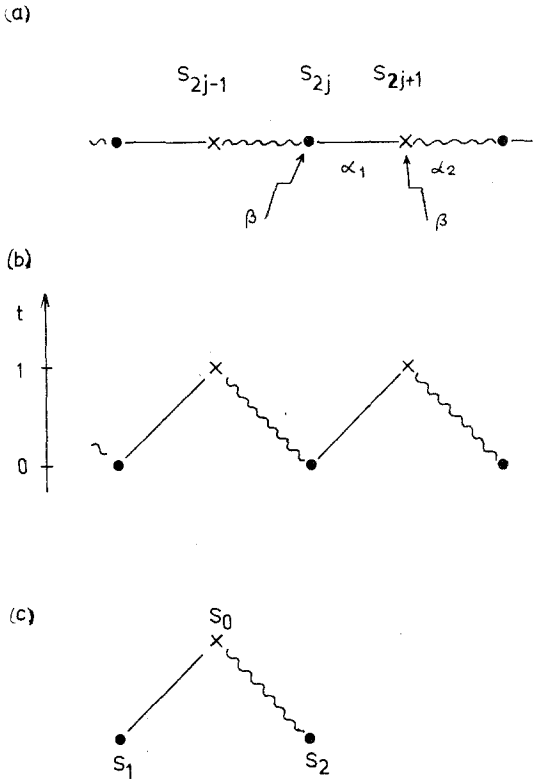

Fig. 1. The one-dimensional Ansatz problem. The even-numbered spins are denoted by dots, the odd-numbered spins by crosses. Wavy lines show α_2, straight lines denote α_1 couplings.

model with alternating nearest-neighbor (NN) interactions in an external magnetic field (see Fig. 1a):

$$-E^A/k_BT = \sum_j (\alpha_1 s_{2j} s_{2j+1} + \alpha_2 s_{2j-1} s_{2j} + \beta s_j) \tag{2.1}$$

Usually it is useful to start with an exactly soluble Ansatz problem, especially if one wants an exact solution along the disorder trajectory. In models with short-range interactions a transfer matrix approach can be used for the calculation of the partition function and the correlation functions. For example, the partition function of the Ansatz (2.1) can be written as

$$Z_{2N}(\alpha_1, \alpha_2, \beta) = \mathrm{Tr}\, T^N \tag{2.2}$$

where

$$T = T_1 T_2$$
$$\langle s|T|s'\rangle = \exp(\alpha_1 s s' + \beta s') \tag{2.3}$$
$$\langle s|T'|s'\rangle = \exp(\alpha_2 s s' + \beta s')$$

In spin representation the elements of T are positive (at most non-negative), therefore the eigenvector $\mathbf{z}$ corresponding to the largest eigenvalue λ_0 of T is positive[11] (nodeless). Define the matrix

$$P = \frac{1}{\lambda_0} Z^{-1} T Z \tag{2.4}$$

where

$$Z_{ik} = z_i \delta_{ik} \tag{2.5}$$

It is trivial to show that the matrix P is stochastic, that is

$$\sum_k P_{ik} = 1 \tag{2.6}$$

and from (2.2)

$$Z_{2N}^{\text{Ising}} = \lambda_0^N \operatorname{Tr} P^N = \lambda_0^N Z_{2N}^{\text{Markov}} \tag{2.7}$$

Here $\lim_{N\to\infty} P^N$ represents the limit distribution of a Markov process defined by P. Note that the spin–spin correlation functions calculated from the Ising and from the Markov representation are exactly the same. This establishes the one-to-one correspondence between the Ansatz (2.1) [see also II Eq. (3.6)] and the Verhagen Ansatz.[6]

Next, one proceeds by constructing a dynamic process leaving invariant the probability distribution $(1/Z)\exp[-(1/k_B T)E^A(s)]$ of a row (layer) of spins. Deform the Ansatz row (see Fig. 1a) into the sawtooth arrangement shown in Fig. 1b. The Ansatz extends now into two rows in the y (time) direction. The stationary distribution of the first ($t = 0$) row can be obtained by summing up every second spin of (2.1)—they are denoted by crosses in Fig. 1b.

Now consider the following game: from left to right place on the second row a spin in the state $+1$ (-1) according to the conditional probability (see Fig. 1c)

$$p(s_0|s_1, s_2) = \frac{\exp\left[s_0(\alpha_1 s_1 + \alpha_2 s_2 + \beta)\right]}{2\cosh(\alpha_1 s_1 + \alpha_2 s_2 + \beta)}$$
$$= \exp\left[s_0(\alpha_1 s_1 + \alpha_2 s_2 + \beta) - A - B_1 s_1 - B_2 s_2 - C s_1 s_2\right] \tag{2.8}$$

where

$$A = \tfrac{1}{4}\ln 2^4 c_1c_2c_3c_4, \qquad B_1 = \tfrac{1}{4}\ln(c_1c_2/c_3c_4)$$

$$B_2 = \tfrac{1}{4}\ln(c_1c_3/c_2c_4), \qquad C = \tfrac{1}{4}\ln(c_1c_4/c_2c_3)$$

$$c_1 = \cosh(\alpha_1 + \alpha_2 + \beta), \qquad c_2 = \cosh(\alpha_1 - \alpha_2 + \beta)$$

$$c_3 = \cosh(\alpha_1 - \alpha_2 - \beta), \qquad c_4 = \cosh(\alpha_1 + \alpha_2 - \beta).$$

Obviously, if the probability distribution of the predecessor spins ($t = 0$ row) is sampled from the equilibrium distribution, so will be the probability of spins on the second row ($t = 1$). When all spins on the second row are set, follow the game with the third, fourth, etc. row. That way one constructs a stochastic crystal where the distribution of spins on sawtooth rows is obtained by solving the Ansatz problem (2.1). Note that the lattice is constructed diagonal-to-diagonal and, as explained in II, leads to the determination of disorder lines.

In the Monte Carlo algorithm[10] following the kinetic Ising model rules[1] only one spin is set in each row, the others remaining fixed (see I). In the game described above, however, every spin of a new row is tested, and this represents an elementary action of the time-evolution operator. The sawtooth arrangement makes the detailed balance requirement (see I) unnecessary by ensuring the stationarity of the equilibrium distribution given by the Ansatz. Although possibly very interesting, the study of the dynamic properties of these crystal growth models is beyond the scope of this paper. The main observation to be made is that the stationary crystals grown from the equilibrium distribution of Ansatz spins can be reinterpreted as a $(d+1)$-dimensional lattice model.[5,6] The form of the energy

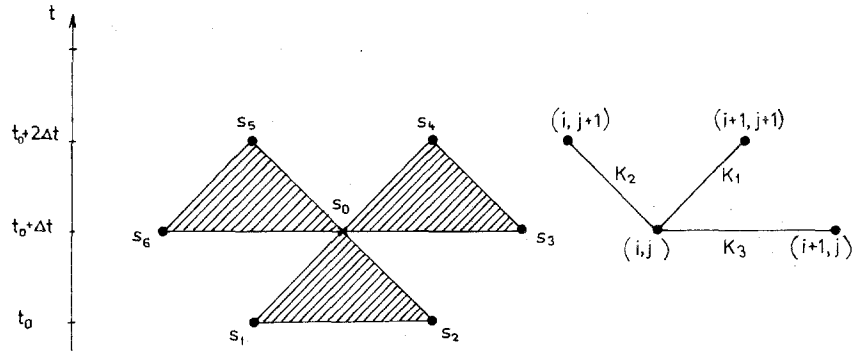

Fig. 2. Construction of the Monte Carlo lattice and the three directions of the triangular lattice.

functional of the latter model is constructed by taking into account all processes during which a given spin s_0 behaves as a new generation spin or as a parent spin. For the Ansatz (2.1) this is shown in Fig. 2. The form of the energy is obtained by grouping together all couplings connected to the central spin s_0. In the example considered here one has to deal with the part $\ldots p(s_0 \mid s_1, s_2)p(s_5 \mid s_6, s_0)p(s_4 \mid s_0, s_3) \ldots$. Using Eq. (2.8) one recognizes a triangular Ising lattice with couplings K_1, K_2, and K_3 given by (see Fig. 2 for notations)

$$\begin{aligned} K_1 &= \alpha_1 \\ K_2 &= \alpha_2 \\ K_3 &= -C \end{aligned} \tag{2.9}$$

in an external field

$$H = \beta - B_1 - B_2 \tag{2.10}$$

where A, C, B_1, and B_2 are given functions of α_1, α_2, and β. From (2.10) the parameter β can be eliminated as

$$\begin{gathered} \cosh 2\beta = \tfrac{1}{2}\left\{ b(a-1) + \left[b^2(a-1)^2 + 4a^2 \right]^{1/2} \right\} \\ a = 2\cosh 2H, \qquad b = \cosh 2(K_1 + K_2) \end{gathered} \tag{2.11}$$

and the disorder constraint is

$$\exp(-4K_3) = \frac{\cosh 2(K_1 + K_2) + \cosh 2\beta}{\cosh 2(K_1 - K_2) + \cosh 2\beta} \tag{2.12}$$

As shown in I and II the correlation functions of spins lying on the same time row or on the sawtooth are calculated as usual from the transfer matrix formalism. One might guess that the free energy per spin can also be calculated from Eqs. (2.1)–(2.2). However, in order to calculate the free energy per spin, f, of the grown crystal, one has to slightly modify the Ansatz problem in such a way as to take into account that the couplings generated by the normalization factor [Eq. (2.8)] acquire a minus sign. In our example the modified problem is defined as

$$\begin{aligned} -E/k_B T = \sum_j \big[& \alpha_1 s_{2j} s_{2j+1} + \alpha_2 s_{2j-1} s_{2j} + \beta s_{2j+1} \\ & - 2C s_{2j} s_{2j+2} + (\beta - 2B_1 - 2B_2) s_{2j} \big] \end{aligned} \tag{2.13}$$

(see also Fig. 3). The free energy per spin is most conveniently calculated by summing first the odd-numbered spins (denoted by crosses in Fig. 3) and then by the transfer matrix method. One may easily see that in the

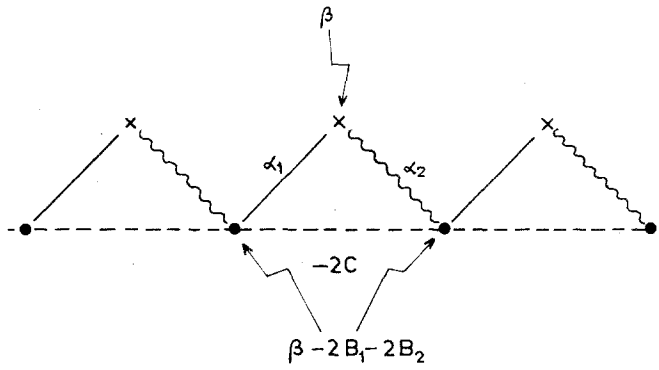

Fig. 3. The modified Ansatz problem for the calculation of the free energy per spin. The dashed line represents a $-2C$ coupling, while the field acting on even (odd) numbered spins is $\beta - 2(B_1 + B_2)$ and β, respectively.

notation of Fig. 2 one has:

$$\begin{aligned} \partial f/\partial K_1 &= \langle s_{i,j}s_{i+1,j+1}\rangle = \langle s_{2j}s_{2j+1}\rangle \\ \partial f/\partial K_2 &= \langle s_{i,j}s_{i+1,j}\rangle = \langle s_{2j-1}s_{2j}\rangle \\ \partial f/\partial K_3 &= \langle s_{i,j}s_{i,j+1}\rangle = \langle s_{2j}s_{2j+2}\rangle \\ \partial f/\partial H &= \langle s_{i,j}\rangle = \langle s_{2j}\rangle \end{aligned} \tag{2.14}$$

and from Eq. (2.13)

$$f \equiv \frac{1}{N}\ln Z_N = \frac{1}{2}A + \frac{1}{2}\ln\left[e^{K_3}\cosh H + (e^{2K_3}\sinh^2 H + e^{-2K_3})^{1/2}\right] \tag{2.15}$$

where A is given in Eq. (2.8). The spin–spin correlations on the $t = \text{const}$ rows are calculated as usual and for $\alpha_1 = \alpha_2$ one obtains

$$\langle s_{i,j}s_{i,j+r}\rangle = a(\lambda_-/\lambda_+)^r \tag{2.16}$$

with a a constant and

$$\begin{aligned} \lambda_\pm &= e^C\cosh(\beta + B) \pm \left[e^{2C}\sinh^2(\beta + B) + e^{-2C}\right]^{1/2} \\ B &= B_1 = B_2 \end{aligned} \tag{2.17}$$

The one-dimensional Ansatz (2.1) has a $T = 0$ ($|\alpha_1|, |\alpha_2|, \beta \to \infty$) Ising-type phase transition if $\beta \leqslant |\alpha_1| + |\alpha_2|$; $\alpha_1, \alpha_2 < 0$. Calculating the corresponding K_1, K_2, K_3, and H couplings it turns out that the disorder subspace (2.12) ends on the line

$$H_{c_1} = 2|K_1| + 2|K_2| - 4|K_3| \qquad (T \to 0) \tag{2.18}$$

which is the critical field value separating the double and the triple degenerate ground states of the anisotropic antiferromagnetic triangular Ising model.[12]

The example shown here was first treated by Verhagen.[6] Finally, we comment on the possibility of analytically continuing these results to complex couplings (negative Boltzmann weights). If $H = 0$, a duality transformation holds between the triangular and the honeycomb Ising model.[13] However, since on the disorder subspace[14] $\operatorname{sgn}(K_1K_2K_3) = -1$, the duality transformation will map the disorder line into an order line of the analytic continuation of the honeycomb lattice (complex couplings), as discussed in II. Another possibility arises from the matrix inversion method.[9] After constructing the diagonal-to-diagonal matrix as in II Section 3, one calculates the inverse of that matrix. Following Baxter[15] one obtains for the free energy per spin

$$f(K_1, K_2, K_3, H) + f(-K_3, K_2 + i\pi/2, -K_1, -H) = \ln 2i \sinh 2K_2 \tag{2.19}$$

Note that for $H = 0$ this relation and a simple relation expressing the invariance of f to lattice rotations are sufficient to solve the model exactly.[9,15]

3. THE EIGHT-VERTEX MODEL REVISITED

The disorder line of the eight-vertex model has been previously discussed in II and independently in Refs. 5 and 16. Enting had also briefly discussed the IRF model.[5] In order to show the flexibility of the crystal growth method we first reconsider here the eight-vertex (the even) model in its most general form. These calculations will be also used when discussing the staggered eight-vertex model (Section 4).

The Ansatz problem is shown in Figs. 4a and 4b. The Ansatz parameters α_1, α_2, α_3, and α_4 correspond to the couplings s_0s_1, s_0s_2, s_0s_3, and $s_0s_1s_2s_3$, respectively. Since the general even (eight-vertex) model has in total five independent couplings, this Ansatz should lead to a four-dimensional disorder subspace. It is also clear that the form of the Ansatz is a straightforward generalization of (2.1). However, here one has to sum up two consecutive rows of spins in order to obtain the basic stationary distribution (see Fig. 4a). Using the notations of Fig. 4b the conditional probability is given as

$$p(s_0 | s_1, s_2, s_3) = \exp\{s_0(\alpha_1 s_1 + \alpha_2 s_2 + \alpha_3 s_3 + \alpha_4 s_1 s_2 s_3) - A - B_1 s_1 s_2 - B_2 s_2 s_3 - B_3 s_1 s_3\} \tag{3.1}$$

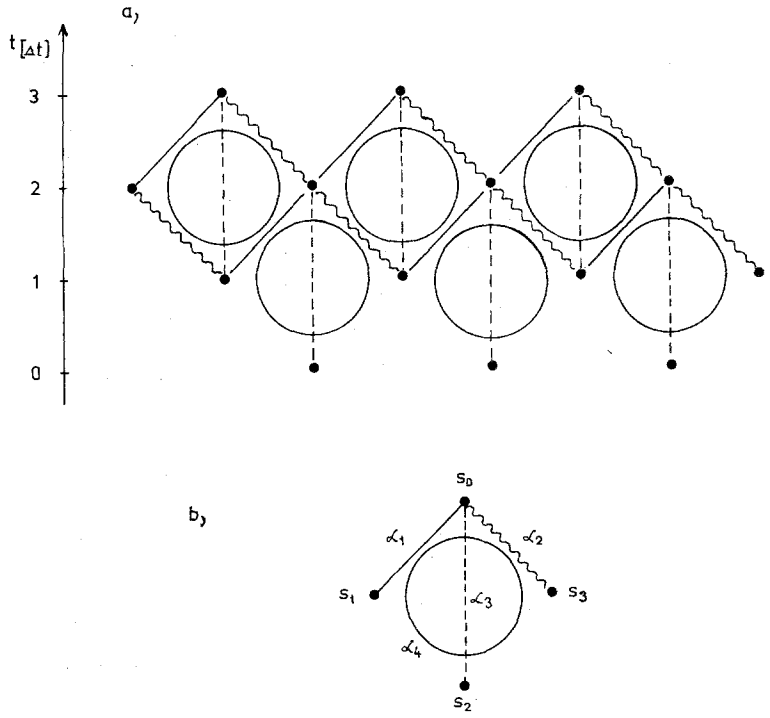

Fig. 4. The Ansatz problem for the eight-vertex problem. The couplings α_1, α_2, α_3, and α_4 are denoted by straight, dashed, wavy, and circle lines, respectively.

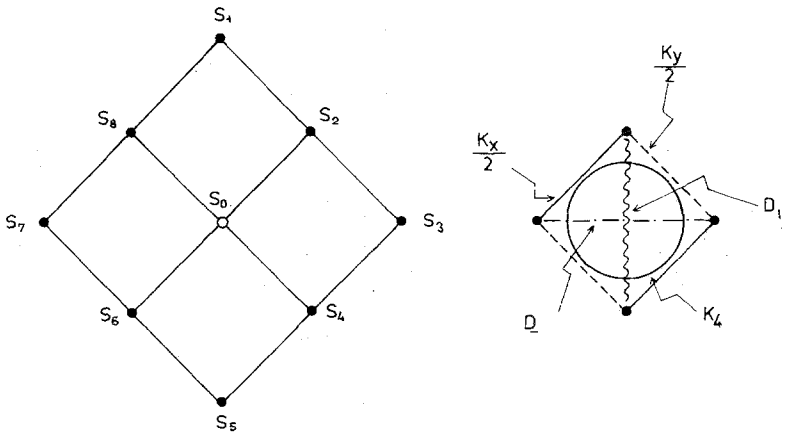

Fig. 5. Construction of the stochastic lattice for the eight-vertex problem.

where

$$\begin{aligned} A &= \tfrac{1}{4}\ln 2^4 c_1c_2c_3c_4, & B_1 &= \tfrac{1}{4}\ln(c_1c_2/c_3c_4) \\ B_2 &= \tfrac{1}{4}\ln(c_1c_3/c_2c_4), & B_3 &= \tfrac{1}{4}\ln(c_1c_4/c_2c_3) \\ c_1 &= \cosh(\alpha_1+\alpha_2+\alpha_3+\alpha_4), & c_2 &= \cosh(\alpha_1+\alpha_2-\alpha_3-\alpha_4) \\ c_3 &= \cosh(\alpha_1-\alpha_2-\alpha_3+\alpha_4), & c_4 &= \cosh(\alpha_1-\alpha_2+\alpha_3-\alpha_4) \end{aligned} \tag{3.2}$$

The crystal is constructed as explained in the previous section and is shown in Fig. 5. By collecting all couplings related to the spin s_0 one obtains an eight-vertex model in the following spin representation (see Fig. 5):

$$\begin{aligned} K_4 &= \alpha_4 \\ D_1 &= \alpha_2 \\ D_- &= -B_3 \\ K_x &= \alpha_1 - B_2 \\ K_y &= \alpha_3 - B_1 \end{aligned} \tag{3.3}$$

The disorder condition can be expressed as

$$\exp(-4D_-) = \frac{\cosh 2(\alpha_1+\alpha_3) + \cosh 2(K_4+D_1)}{\cosh 2(\alpha_1-\alpha_3) + \cosh 2(K_4-D_1)} \tag{3.4}$$

where

$$\begin{aligned} \cosh 2(\alpha_1 \pm \alpha_3) &= \tfrac{1}{2}\left\{ b_\pm(a_\pm - 1) + \left[b_\pm^2(a_\pm-1)^2 + 4a_\pm^2 \right]^{1/2} \right\} \\ a_\pm &= 2\cosh 2(K_x \pm K_y) \\ b_\pm &= \cosh 2(K_4 \pm D_1) \end{aligned} \tag{3.5}$$

Equation (3.4) is a single condition between the five independent couplings of the eight-vertex model. This result extends the similar calculations of Refs. 5, 3, and 16, which were obtained for more symmetric cases. The calculation of the free energy and of the correlation functions is lengthy and is left to Appendix A. The correlation functions between two spins on the same time-row has the form

$$\langle s_0 s_r \rangle = \tilde{A}(\lambda_3/\lambda_1)^r + \tilde{B}(\lambda_4/\lambda_1)^r \tag{3.6}$$

if λ_3 and λ_4 are real [see Eqs. (A.10)–(A.11)] or

$$\langle s_0 s_r \rangle = \tilde{C}\left(\frac{\lambda^{\text{odd}}}{\lambda_1} \right)^r \cos(qr+\varphi) \tag{3.7}$$

if λ_3 and λ_4 form a complex conjugated pair. It turns out that by changing the Ansatz parameters $\alpha_1, \ldots, \alpha_4$ one can observe within the disorder

surface (3.4) a "one-dimensional" disorder subspace defined by Eq. (A.13), where the correlation length has a strong cusplike minimum. Therefore it is possible to monitor the change from monotonic to a modulated decay within the exactly soluble disorder subspace (3.4). This result strongly supports the conjectures made in I regarding the nature and the physical properties of systems with competing interactions near a disorder line. Note that the case $K_x = K_y$ discussed in II shows a single exponential decay of the correlations.

Finally, we briefly discuss the possible analytic continuations of these results. As shown in II Table II the general eight-vertex model (3.3) can be expressed in the "diagonal-to-diagonal" transfer matrix representation in terms of the coefficients $P_{J_2}^{J_1 J_3}$ [II(3.5)]. The duality transformation [II(3.12)] and the use of II Table I lead to the dual model, with some of the weights assigning negative values.

Alternately, in the matrix inversion method a straightforward calculation leads to

$$f(K_x, K_y, D_1, D_-, K_4) + f(\tilde{K}_x, \tilde{K}_y, \tilde{D}_1, \tilde{D}_-, \tilde{K}_4) = \tilde{a} \tag{3.8}$$

where

$$\begin{aligned}
\tilde{K}_x &= -K_y \\
\tilde{K}_y &= -K_x \\
\tilde{D}_1 &= D_1 + i\frac{\pi}{2}\frac{n+m}{2}, \qquad n, m = \pm 1, \pm 2, \ldots \\
\tilde{D}_- &= \tfrac{1}{2}\ln\left[\sinh 2(D_1 - K_4)/\sinh 2(D_1 + K_4)\right] \\
\tilde{K}_4 &= K_4 + i\frac{\pi}{2}\frac{n-m}{2} \\
\tilde{a} &= D_- + \tfrac{1}{2}\ln\left[2^2 \sinh(D_1 + K_4)\sinh(K_4 - D_-)\right]
\end{aligned} \tag{3.9}$$

It would be interesting to clarify what is the relation between the two analytic continuations, one generated by the duality transformation II(3.12) and the other one by the matrix inversion (3.9).

4. THE STAGGERED EIGHT-VERTEX MODEL

The next step towards more and more complex models is the staggered eight-vertex model. In the Hamiltonian limit this model had already been discussed in I. Here, again, the crystal growth method allows for a straightforward generalization of results. The Ansatz problem is shown in Fig. 6, while the construction of the crystal is sketched in Fig. 7. The results obtained for the homogeneous eight-vertex model are easily generalized by

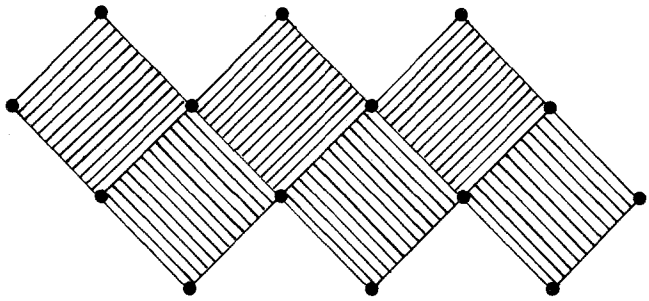

Fig. 6. Schematic representation of the Ansatz for the staggered model.

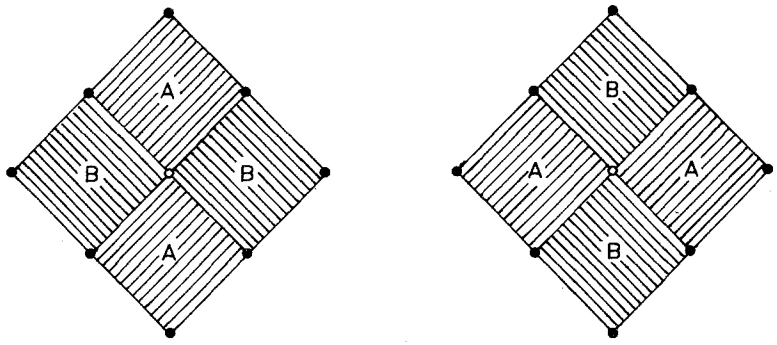

Fig. 7. The two basic processes for the construction of the staggered lattice.

introducing a sublattice index $i = A, B$:

$$
\begin{aligned}
K_4^{(i)} &= \alpha_4^{(i)} \\
D_1^{(i)} &= \alpha_2^{(i)} \\
K_{06} = K_x^{(i,j)} &= \alpha_1^{(i)} - B_2^{(j)}, \qquad K_{02} = K_x^{(j,i)} \\
K_{08} = K_y^{(i,j)} &= \alpha_3^{(i)} - B_1^{(j)}, \qquad K_{04} = K_y^{(j,i)} \\
D_-^{(i)} &= -B_3^{(i)}
\end{aligned}
\tag{4.1}
$$

where $i = A, B$, $i \neq j$, and $K_{02} \ldots$ corresponds to the coupling between s_0 and $s_2 \ldots$, as shown in Figs. 5 and 7. The disorder conditions are more complicated:

$$
\exp\left(-4D_-^{(i)}\right) = \frac{\cosh 2\left(\alpha_1^{(i)} + \alpha_3^{(i)}\right) + \cosh 2\left(K_4^{(i)} + D_1^{(i)}\right)}{\cosh 2\left(\alpha_1^{(i)} - \alpha_3^{(i)}\right) + \cosh 2\left(K_4^{(i)} - D_1^{(i)}\right)}, \qquad i = A, B \tag{4.2}
$$

where now

$$\cosh 2\left(\alpha_1^{(i)} \pm \alpha_3^{(i)}\right) = \tfrac{1}{2}\left[c_{\pm}^{(i)} + \left(c_{\pm}^{(i)2} + 4d_{\pm}^{(i)}\right)^{1/2}\right] \tag{4.3}$$

$$\begin{aligned} c^{(i)} &= (ab\bar{a}\bar{b} + \bar{a} - b\bar{b} - a)/(ab + \bar{b}) \\ d^{(i)} &= (\bar{a}b + a\bar{a}\bar{b})/(ab + \bar{b}) \end{aligned} \tag{4.4}$$

and

$$\begin{aligned} a_{\pm} &= 2\cosh 2\left(K_x^{(i,j)} \pm K_y^{(i,j)}\right) \\ \bar{a}_{\pm} &= 2\cosh 2\left(K_x^{(j,i)} \pm K_y^{(j,i)}\right) \\ b_{\pm} &= \cosh 2\left(K_4^{(i)} \pm D_1^{(i)}\right) \\ \bar{b}_{\pm} &= \cosh 2\left(K_4^{(j)} \pm D_1^{(j)}\right) \end{aligned} \tag{4.5}$$

In Eqs. (4.4) the $\pm$ subscript had been omitted on both sides of the equations. Obviously, the general staggered eight-vertex model has ten independent couplings and is exactly soluble on an eight-dimensional subspace defined by Eqs. (4.2)–(4.5). We consider now a few special cases.

4.1. The Union-Jack Lattice

As shown in Fig. 8 the Union-Jack lattice is obtained if for the $\odot$ spin one has

$$\begin{aligned} \alpha_4^{(i)} &= 0 \\ \alpha_2^{(A)} &= 0 \\ B_3^{(B)} &= 0 \end{aligned} \tag{4.6}$$

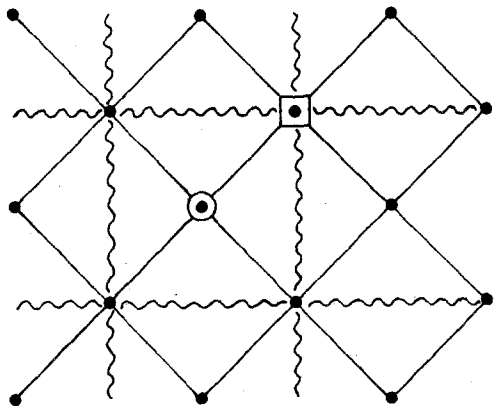

Fig. 8. The Union-Jack lattice. The spins denoted by $\odot$ and $\boxdot$ correspond to the two possible processes shown in Fig. 7.

These restrictions lead to a very general Union-Jack lattice with a maximal number of six independent couplings. Originally, the model was solved[17] for the case when the diagonal interactions through the central spin are all equal and the original Ising couplings (wavy lines in Fig. 8) are also isotropic. The Union-Jack lattice is a free fermion model and the correlation functions can be calculated exactly. The disorder point had been found by Stephenson.[14] Here Eqs. (4.2)–(4.7) generalize his result to the most general Union-Jack lattice.

4.2. The ANNNI Model

The axial-next-nearest-neighbor Ising (ANNNI) model[18] can be reformulated as a staggered eight-vertex model[19] and is shown in Fig. 9. Again, it is easy to see that one has to satisfy the following conditions:

$$\alpha_4^{(i)} = 0 \tag{4.7}$$

while for the $\odot$ spin

$$\begin{aligned} \alpha_3^{(B)} - B_1^{(A)} &= 0 \\ \alpha_1^{(B)} - B_2^{(A)} &= 0 \end{aligned} \tag{4.8}$$

and

$$\alpha_1^{(A)} - B_2^{(B)} = \alpha_3^{(A)} - B_1^{(B)} \neq 0$$

Also one has the condition

$$\begin{aligned} \alpha_2^{(A)} &= \alpha_2^{(B)} \\ B_3^{(A)} &= B_3^{(B)} \end{aligned} \tag{4.9}$$

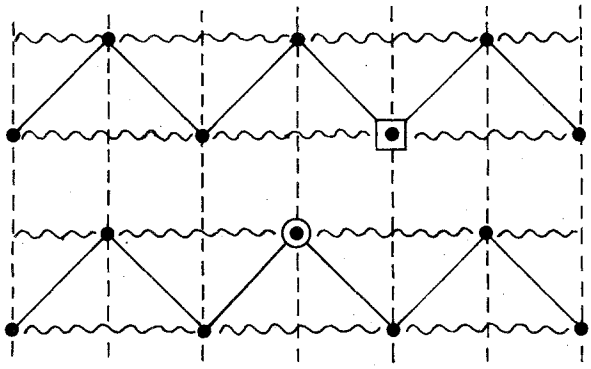

Fig. 9. The ANNNI model as a staggered eight-vertex model. The Ising couplings in the x, y directions are denoted by solid and dashed lines, while the axial NNN interaction is denoted by wavy lines.

The ANNNI model has three independent couplings and since the three equations (4.8) are not independent, one obtains a two-dimensional disorder subspace. Its calculation is done, however, more easily from the transfer matrix formulation.[3]

4.3. The Ashkin–Teller Model

It is well known that the Ashkin–Teller (AT) model[20] can be expressed as the staggered eight-vertex model shown in Fig. 10. The eight-vertex couplings are given by

$$
\begin{aligned}
D_1^{(i)} &= \tilde{K}_2^{(i)} + \frac{1}{4}\ln\frac{\sinh 2\left(\tilde{K}_2^{(i)} + \tilde{K}_4^{(i)}\right)}{\sinh 2\left(\tilde{K}_2^{(i)} - \tilde{K}_4^{(i)}\right)} \\
D_{-}^{(i)} &= -\tfrac{1}{4}\ln\left[\tanh\left(\tilde{K}_2^{(i)} + \tilde{K}_4^{(i)}\right)\tanh\left(\tilde{K}_2^{(i)} - \tilde{K}_4^{(i)}\right)\right] \\
K_4^{(i)} &= \tfrac{1}{4}\ln\left[\tanh\left(\tilde{K}_2^{(i)} - K_4^{(i)}\right)/\tanh\left(\tilde{K}_2^{(i)} + K_4^{(i)}\right)\right]
\end{aligned}
\tag{4.10}
$$

where $\tilde{K}_2^{(i)}, \tilde{K}_4^{(i)}$ are the original AT couplings in spin representation and $i = x, y$:

$$
-\frac{H^{\mathrm{AT}}}{k_B T} = \tilde{K}_2^{(x,y)} \sum_{\langle ij\rangle_{x,y}} (s_i s_j + \tau_i \tau_j) + \tilde{K}_4^{(x,y)} \sum_{\langle ij\rangle_{x,y}} s_i s_j \tau_i \tau_j \tag{4.11}
$$

s_i and τ_i are Ising variables ± 1 and $\langle i, j\rangle_{x,y}$ denotes nearest neighbors in

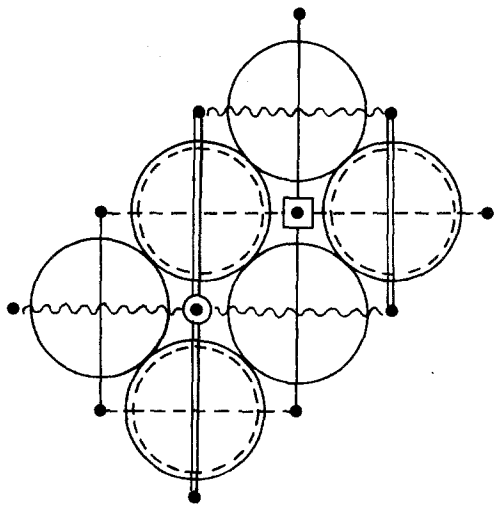

Fig. 10. The Ashkin–Teller model as a staggered eight-vertex model. For details, see text.

the x (y) direction. If the additional constraints

$$\begin{aligned} \alpha_1^{(i)} - B_2^{(j)} &= 0 \\ \alpha_3^{(i)} - B_1^{(j)} &= 0 \end{aligned} \tag{4.12}$$

are met one gains the disorder solution. A simpler derivation of this result is given in Section 7, where it is also shown that (4.2) do not lead to a disorder line for positive Boltzmann weights on a square lattice.

5. THE IRF AND THE SIXTEEN-VERTEX MODEL

The interactions-around-a-face (IRF) model has been briefly considered before.[5,3,16] The sixteen-vertex model can be represented as a staggered IRF model.[23] In general, the IRF model contains five independent couplings for odd and five other couplings corresponding to even spin products. As already shown by Enting,[5] the disorder subspace forms an eight-dimensional subspace. Unfortunately, the form of the two constraints in terms of IRF couplings is quite frightful and will not be given here. The calculation of the free energy and of correlation functions follows the line of thought of Appendix A but involves the diagonalization of an irreducible 4×4 matrix. Therefore, I shall restrict myself here to a minimal description, though sufficient for numerical purposes.

One starts again with an Ansatz as displayed in Fig. 7. However, the conditional probability $p(s_0 | s_1, s_2, s_3)$ has its most general form

$$\begin{aligned} p^{(i)}(s_0 | s_1, s_2, s_3) = \exp\{ s_0[& \beta_1^{(i)} + \beta_2^{(i)} s_1 s_2 + \beta_3^{(i)} s_2 s_3 + \beta_4^{(i)} s_1 s_3 \\ & + \alpha_1^{(i)} s_1 + \alpha_2^{(i)} s_2 + \alpha_3^{(i)} s_3 + \alpha_4^{(i)} s_1 s_2 s_3] \\ & - A^{(i)} - D_1^{(i)} s_1 - D_2^{(i)} s_2 - D_3^{(i)} s_3 - B_1^{(i)} s_1 s_2 \\ & - B_2^{(i)} s_2 s_3 - B_3^{(i)} s_1 s_3 - E^{(i)} s_1 s_2 s_3 \} \end{aligned} \tag{5.1}$$

where

$$\begin{aligned} A &= \tfrac{1}{8} \ln 2^8 c_1 c_2 c_3 c_4 c_5 c_6 c_7 c_8 \\ D_1 &= \tfrac{1}{8} \ln(c_1 c_3 c_4 c_7 / c_2 c_5 c_6 c_8) \\ D_2 &= \tfrac{1}{8} \ln(c_1 c_2 c_4 c_6 / c_3 c_5 c_7 c_8) \\ D_3 &= \tfrac{1}{8} \ln(c_1 c_2 c_3 c_5 / c_4 c_6 c_7 c_8) \\ B_1 &= \tfrac{1}{8} \ln(c_1 c_4 c_5 c_8 / c_2 c_3 c_6 c_7) \\ B_2 &= \tfrac{1}{8} \ln(c_1 c_2 c_7 c_8 / c_3 c_4 c_5 c_6) \\ B_3 &= \tfrac{1}{8} \ln(c_1 c_3 c_6 c_8 / c_2 c_4 c_5 c_7) \\ E &= \tfrac{1}{8} \ln(c_1 c_5 c_6 c_7 / c_2 c_3 c_4 c_8) \end{aligned} \tag{5.2}$$

and

$$
\begin{aligned}
c_1 &= 2\cosh(\beta_1+\beta_2+\beta_3+\beta_4+\alpha_1+\alpha_2+\alpha_3+\alpha_4)\\
c_2 &= 2\cosh(\beta_1-\beta_2+\beta_3-\beta_4-\alpha_1+\alpha_2+\alpha_3-\alpha_4)\\
c_3 &= 2\cosh(\beta_1-\beta_2-\beta_3+\beta_4+\alpha_1-\alpha_2+\alpha_3-\alpha_4)\\
c_4 &= 2\cosh(\beta_1+\beta_2-\beta_3-\beta_4+\alpha_1+\alpha_2-\alpha_3-\alpha_4)\\
c_5 &= 2\cosh(\beta_1+\beta_2-\beta_3-\beta_4-\alpha_1-\alpha_2+\alpha_3+\alpha_4)\\
c_6 &= 2\cosh(\beta_1-\beta_2-\beta_3+\beta_4-\alpha_1+\alpha_2-\alpha_3+\alpha_4)\\
c_7 &= 2\cosh(\beta_1-\beta_2+\beta_3-\beta_4+\alpha_1-\alpha_2-\alpha_3+\alpha_4)\\
c_8 &= 2\cosh(\beta_1+\beta_2+\beta_3+\beta_4-\alpha_1-\alpha_2-\alpha_3-\alpha_4)
\end{aligned}
\tag{5.3}
$$

In (5.2)–(5.3) the upper sublattice index (i) has been omitted in order to not add further complications to these formulas.

From Figs. 5 and 7 and the form ((5.1) one obtains the couplings of the staggered IRF model at the disorder line (in parentheses are the spin products denoted according to Fig. 5):

$$(s_0) \qquad H^{(i)} = \beta_1^{(i)} - D_1^{(j)} - D_2^{(i)} - D_3^{(j)} \tag{5.4a}$$

$$(s_0 s_1, s_0 s_5) \qquad D_1^{(i)} = \alpha_2^{(i)} \tag{5.4b}$$

$$(s_0 s_3, s_0 s_7) \qquad D_{-}^{(j)} = -B_3^{(j)} \tag{5.4c}$$

$$
\begin{aligned}
(s_0 s_2) \qquad & K_x^{(j,i)} = \alpha_1^{(j)} - B_2^{(i)}\\
(s_0 s_6) \qquad & K_x^{(i,j)} = \alpha_1^{(i)} - B_2^{(j)}
\end{aligned}
\tag{5.4d}
$$

$$
\begin{aligned}
(s_0 s_8) \qquad & K_y^{(j,i)} = \alpha_3^{(j)} - B_1^{(i)}\\
(s_0 s_4) \qquad & K_y^{(i,j)} = \alpha_3^{(i)} - B_1^{(j)}
\end{aligned}
\tag{5.4e}
$$

$$
\begin{aligned}
(s_0 s_1 s_2, s_0 s_4 s_5) \qquad & K_{3-1}^{(i)} = \beta_3^{(i)}\\
(s_0 s_6 s_8) \qquad & K_{3-1}^{(j)} = \beta_3^{(j)}
\end{aligned}
\tag{5.4f}
$$

$$
\begin{aligned}
(s_0 s_1 s_8, s_0 s_5 s_6) \qquad & K_{3-2}^{(i)} = \beta_2^{(i)}\\
(s_0 s_2 s_4) \qquad & K_{3-2}^{(j)} = \beta_2^{(j)}
\end{aligned}
\tag{5.4g}
$$

$$
\begin{aligned}
(s_0 s_3 s_4, s_0 s_6 s_7) \qquad & K_{3-3}^{(j)} = -E^{(j)}\\
(s_0 s_2 s_8) \qquad & K_{3-3}^{(i)} = -E^{(i)}
\end{aligned}
\tag{5.4h}
$$

$$
\begin{aligned}
(s_0 s_2 s_3, -s_0 s_7 s_8) \qquad & K_{3-4}^{(j)} = \beta_4^{(j)}\\
(s_0 s_4 s_6) \qquad & K_{3-4}^{(i)} = \beta_4^{(i)}
\end{aligned}
\tag{5.4i}
$$

$$K_4^{(i)} = \alpha_4^{(i)} \tag{5.4j}$$

Using Eqs. (5.2)–(5.4) one has first to express the Ansatz parameters in terms of the staggered IRF parameters. This means to solve Eqs. (5.4a), (5.4d), and (5.4e) for $\beta_1^{(i)}$, $\alpha_1^{(i)}$, and $\alpha_3^{(i)}$. The disorder constraints are given by Eqs. (5.4c), (5.4h). Finally one obtains an exact solution in a 16-dimensional subspace of a 20-dimensional parameter space of the staggered IRF model.

The sixteen-vertex model is defined in such a way[23] that, say, $\alpha_i^{(A)} = \beta_i^{(A)} = 0$; $i = 1, \ldots 4$. For the homogeneous IRF model $\alpha_i^{(A)} = \alpha_i^{(B)}$; $\beta_i^{(A)} = \beta_i^{(B)}$, $i = 1, \ldots, 4$. In both cases one can solve the model in an eight-dimensional subspace of its ten-dimensional parameter space. The free energy and the correlation functions can be calculated following the procedure shown in Appendix A. However, the even and the odd sector are not perpendicular any longer. This implies correlation functions of the form

$$\langle s_0 s_r \rangle = \langle s \rangle^2 + a_1 \left(\frac{\lambda_2}{\lambda_1} \right)^r + a_2 \left(\frac{\lambda_3}{\lambda_1} \right)^r + a_3 \left(\frac{\lambda_4}{\lambda_1} \right)^r \tag{5.5}$$

where at least λ_1 and λ_2 are real eigenvalues. Again, it is possible to monitor a change from the (5.5) form to

$$\langle s_0 s_r \rangle = \langle s \rangle^2 + a \left(\frac{\tilde{\lambda}}{\lambda_1} \right)^r \cos(qr + \varphi) + b \left(\frac{\lambda_2}{\lambda_1} \right)^r \tag{5.6}$$

where $\lambda_{3,4} = \tilde{\lambda} e^{\pm iqr}$, $\tilde{\lambda} > \lambda_2$.

These general remarks end the part dealing with white and black crystals (Ising variables). We shall try to make the next section more colorful.

6. GROWING COLORED CRYSTALS: POTTS MODELS ON A TRIANGULAR LATTICE

The crystal growth models treated so far were all related to Ising variables: a spin value -1 means that an atom is absent, $+1$ means that it is present in a given lattice point. The procedure can be generalized to take into account atoms of different species (colors) described by a Potts-like variable $l_i = 0, 1, 2, \ldots, q-1$.

Let us start with an Ansatz of the type discussed in Section 2 (see Fig. 1). The energy function of the Ansatz problem is now given by

$$-\frac{E^A}{k_B T} = \sum_j \left[\alpha_1 \delta_{l_{2j}, l_{2j+1}} + \alpha_2 \delta_{l_{2j-1}, l_{2j}} + \beta_0 \left(\delta_{l_{2j},0} + \delta_{l_{2j+1},0} \right) \right.$$

$$\left. + \beta_1 \delta_{l_{2j}, l_{2j+1}} \delta_{l_{2j},0} + \beta_2 \delta_{l_{2j-1}, l_{2j}} \delta_{l_{2j},0} + \gamma \delta_{l_{2j-1}, l_{2j}} \delta_{l_{2j-2}, l_{2j-1}} \right] \tag{6.1}$$

where

$$\delta_{x,y} = \begin{cases} 1 & \text{if } x = y \\ 0 & \text{if } x \neq y \end{cases}$$

$l_j = 0, 1, \ldots, q-1$. This model corresponds to a one-dimensional staggered Potts model[23] (α_1, α_2) with a field and a two-spin field in the 0 direction $(\beta_0, \beta_1, \beta_2)$ as well as with a three-spin interaction (γ) among odd sites and their nearest neighbors. The normalization factor of the conditional probability can be expressed as (see Fig. 1c)

$$\sum_{l_0} \exp\left[-\frac{1}{k_B T} E(l_0, l_1, l_2) \right] = \exp\left[A + B\delta_{l_1,l_2} + C_1\delta_{l_1,0} + C_2\delta_{l_2,0} + D\delta_{l_1,l_2}\delta_{l_1,0} \right] \tag{6.2}$$

where

$$\begin{aligned} A &= \ln(e^{\alpha_1} + e^{\alpha_2} + e^{\beta_0} + q - 3) \\ B &= \ln\left[(e^{\alpha_1+\alpha_2+\gamma} + e^{\beta_0} + q - 2)/(e^{\alpha_1} + e^{\alpha_2} + e^{\beta_0} + q - 3) \right] \\ C_1 &= \ln\left[(e^{\alpha_1+\beta_0+\beta_1} + e^{\alpha_2} + q - 2)/(e^{\alpha_1} + e^{\alpha_2} + e^{\beta_0} + q - 3) \right] \\ C_2 &= \ln\left[(e^{\alpha_2+\beta_0+\beta_2} + e^{\alpha_1} + q - 2)/(e^{\alpha_1} + e^{\alpha_2} + e^{\beta_0} + q - 3) \right] \\ D &= \ln\left[(e^{\alpha_1+\alpha_2+\beta_0+\beta_1+\beta_2+\gamma} + q - 1)/(e^{\alpha_1} + e^{\alpha_2} + e^{\beta_0} + q - 3) \right] \\ &\quad - B - C_1 - C_2 \end{aligned} \tag{6.3}$$

Using the notation of Fig. 2 the resulting lattice is a Potts model on a triangular lattice with the following couplings:

$$\begin{aligned} K_1 &= \alpha_1 \\ K_2 &= \alpha_2 \\ K_3 &= -B \\ H &= \beta_0 - C_1 - C_2 \\ M_1 &= \beta_1 \\ M_2 &= \beta_2 \\ M_3 &= -D \\ L &= \gamma \end{aligned} \tag{6.4}$$

Note that the K_i, M_i couplings follow the basic directions of the lattice as shown in Fig. 2 but the three-body interaction L is present only for the up-pointing triangles. $x = \exp(\beta_0)$ can be calculated as the positive real

root of the equation

$$x^3 + x^2(2a - fbd) + x(a^2 - fbe - fcd) - fce = 0 \tag{6.5}$$

where

$$\begin{aligned} a &= e^{K_1} + e^{K_2} + q - 3 \\ b &= e^{K_1} + M_1 \\ c &= e^{K_2} + q - 2 \\ d &= e^{K_2 + M_2} \\ e &= e^{K_1} + q - 2, \\ f &= e^{H} \end{aligned} \tag{6.6}$$

The disorder constraints are defined by

$$\begin{aligned} K_3 &= -B(K_1, K_2, M_1, M_2, H, L) \\ M_3 &= -D(K_1, K_2, M_1, M_2, H, L) \end{aligned} \tag{6.7}$$

The free energy and the correlation functions are calculated in Appendix B. If one considers only the Potts interactions ($\beta_0 = \beta_1 = \beta_2 = \gamma = 0$), Eq. (6.7) has a remarkably simple form:

$$\exp(-K_3) = (e^{K_1 + K_2} + q - 1)/(e^{K_1} + e^{K_2} + q - 2) \tag{6.8}$$

This is the generalization of Stephenson's result[14] for the triangular Ising model. Not surprisingly, it follows from (6.8) that in order to get a disorder line one must have competing interactions

$$\operatorname{sgn}(K_1 K_2 K_3) = -1 \tag{6.9}$$

It is interesting to remark that for the isotropic antiferromagnet ($K_1 = K_2 = K_3 = -|K|$) the disorder subspace breaks up in two (real) points

$$e^{-|K|} = 1 \qquad (T = \infty) \tag{6.10}$$

$$e^{-|K|} = \tfrac{1}{2}\left\{-1 + \left[1 + 4(2 - q)\right]^{1/2}\right\} \qquad q \leqslant 2 \tag{6.11}$$

For $q = 2$ it is known that the critical point of the model is depressed to $T = 0$ by the "fully frustration" condition (6.9). At the same time the ground state is macroscopically degenerated and includes the ground-state possibility represented by the one-dimensional Ansatz (6.1). This explains the additional solution (6.11). If $q > 2$ the condition (6.9) does not ensure any more that the system is frustrated and the solution (6.11) becomes complex. For $q < 2$, however, the solution (6.11) corresponds to a nonzero disorder point. In the Ising model ($q = 2$) a systematic analysis of the

correlations in diagonally layered Ising models[25] shows that in the case of competing interactions $0 < T_c < T_D$, where T_c is the (Ising type) critical point and T_D the disorder point. For fully frustrated cases, however, $T_c = T_D = 0$. If one assumes this mechanism to be also valid for $q < 2$, our result (6.11) indicates that the critical point moves away from $T = 0$. An interesting proposition concerning the nature of this phase transition and the structure of the low-temperature phase had been put forward by Berker and Kadanoff.[26]

If $L \neq 0$ Eqs. (6.4) define a self-dual model [see Ref. 24 Eqs. (2.18)–(2.27) and the references mentioned therein]. The duality relation[24] is

$$\frac{e^{K_i^*} - 1}{e^{K_i} - 1} = \frac{q}{z}, \qquad zz^* = q^2, \qquad i = 1,2,3$$
$$z = e^{K_1+K_2+K_3+L} - e^{K_1} - e^{K_2} - e^{K_3} + 2 \tag{6.12}$$

and maps the disorder surface

$$\exp(-K_3) = (e^{K_1+K_2+L} + q - 1)/(e^{K_1} + e^{K_2} + q - 2) \tag{6.13}$$

into an order surface (see also II).

When $L = 0$ but not the fields β_0, β_1, and β_2, the resulting Potts model can be related to different random geometric problems as the percolation problem, the lattice animal problem, etc.[24] Possible applications of these results will be discussed in a separate publication.

7. GENERAL $Z(q)$ MODELS ON A TRIANGULAR LATTICE

Consider the most general nearest-neighbor interaction which is invariant under the transformation $l_{\mathbf{r}} \to l_{\mathbf{r}} + 1$ for all lattice points $\mathbf{r}$, $l_r = 0, 1, \ldots, q-1$. The interaction between two NN spins situated on the direction $i = 1,2,3$ of the triangular lattice can be expanded on Fourier series as

$$-\frac{H^{(q)}}{k_B T} = \sum_{\langle \mathbf{r},\mathbf{r}^1 \rangle} \sum_i \sum_{m=0}^{q-1} \left[c_m^{(i)} \cos m\beta(l_{\mathbf{r}} - l_{\mathbf{r}^1}) + s_m^{(i)} \sin m\beta(l_{\mathbf{r}} - l_{\mathbf{r}^1}) \right] \tag{7.1}$$

where $\langle \mathbf{r}, \mathbf{r}^1 \rangle_i$ are NN lattice sites in direction i, $\beta = 2\pi/q$, $c_m^{(i)}$ and $s_m^{(i)}$ are real couplings obeying

$$c_{q-m}^{(i)} = c_m^{(i)}$$
$$s_{q-m}^{(i)} = -s_m^{(i)} \tag{7.2}$$

The model (7.1) contains as special cases different chiral (asymmetric) Potts[27] and clock[28] models as well as the $Z(q)$ model ($s_m^{(i)} = 0$), the Potts

model,[23] the vector (or planar) Potts model[24] ($s_m^{(i)} = 0$ for all m, $c_m^{(i)} = 0$ if $m \geqslant 2$), the discrete Villain model,[29] etc. In order to obtain general formulas for the disorder–disorder line of (7.1), one starts with an Ansatz as shown in Fig. 1 and with the interaction

$$-\frac{E^A}{k_B T} = \sum_j \sum_{m=0}^{q-1} \left[\alpha_m^{(1)} \cos m\beta(l_{2j+1} - l_{2j}) + \beta_m^{(1)} \sin m\beta(l_{2j+1} - l_{2j}) \right.$$
$$\left. + \alpha_m^{(2)} \cos m\beta(l_{2j} - l_{2j-1}) + \beta_m^{(2)} \sin m\beta(l_{2j} - l_{2j-1}) \right] \tag{7.3}$$

where $\alpha_m^{(i)}$, $\beta_m^{(i)}$ satisfy the condition (7.2). The only nontrivial part of the calculation is to construct the normalization factor of the conditional probability $p(l_0 | l_1, l_2)$ of Fig. 2. Since this is simply an iteration[13] (or decimation) transformation one may use the one-dimensional transfer matrix to obtain the resulting couplings between the spins l_1 and l_2. The one-dimensional transfer matrix between the spins l_1 and l_0 has the continuant form

$$t_{1\to 0} = \begin{bmatrix} f_0 & f_1 & \cdots & & f_{q-1} \\ f_{q-1} & f_0 & f_1 & \cdots & f_{q-2} \\ \vdots & & & & \\ f_1 & f_2 & \cdots & & f_0 \end{bmatrix} \tag{7.4}$$

where

$$f_\rho = \exp\left\{ \sum_m \left[\alpha_m^{(1)} \cos m\beta\rho + \beta_m^{(1)} \sin m\beta\rho \right] \right\} \tag{7.5}$$

The corresponding matrix between the spins l_0 and l_2 has the same structure but with elements given by

$$g_\rho = \exp\left\{ \sum_m \left[\alpha_m^{(2)} \cos m\beta\rho + \beta_m^{(2)} \sin m\beta\rho \right] \right\} \tag{7.6}$$

Summing the spin l_0 corresponds to the matrix multiplication

$$t_{1\to 2} = t_{1\to 0} t_{0\to 2} \tag{7.7}$$

where $t_{1\to 2}$ is also a continuant matrix whose elements are

$$h_\rho = \sum_{\gamma=0}^{q-1} f_\gamma g_{\gamma+\rho} \tag{7.8}$$

The couplings $(\alpha_m^{(3)}, \beta_m^{(3)})$ and the multiplicative constant A of the l_1–l_2

interaction are

$$\begin{aligned} A &= \frac{1}{q}\sum_{\rho} \ln h_\rho \\ -\alpha_m^{(3)} &= \frac{1}{q}\sum_{\rho} \cos m\beta\rho \ln h_\rho \\ -\beta_m^{(3)} &= \frac{1}{q}\sum_{\rho} \sin m\beta\rho \ln h_\rho \end{aligned} \tag{7.9}$$

Since by definition f_ρ and g_ρ are positive [Eqs. (7.5)–(7.6)] so is h_ρ. Hence $\alpha_m^{(3)}$, $\beta_m^{(3)}$ and A are real quantities. The couplings of the general $Z(q)$ model (7.1) are then

$$\begin{aligned} c_m^{(i)} &= \alpha_m^{(i)} \\ s_m^{(i)} &= \beta_m^{(i)}, \qquad i = 1,2,3 \end{aligned} \tag{7.10}$$

and the disorder subspace is given through Eqs. (7.5)–(7.9). In general, the anisotropic model (7.1) has a parameter space whose dimension equals $3(q-1)$. The disorder surface (7.9) is $2(q-1)$ dimensional. Note that except for the trivial one-dimensional case ($\alpha_m^{(i)} = \beta_m^{(i)} = 0$ for $i = 1,2$, any m) the nonstaggered square lattice does not have a disorder solution. The free energy per spin of the model is obtained as

$$f = \tfrac{1}{2}A + \tfrac{1}{2}\ln\left[\sum_{\rho} f_\rho\left(\alpha_m^{(3)}, \beta_m^{(3)}\right)\right] \tag{7.11}$$

where $A(\alpha_m^{(1)}, \alpha_m^{(2)}, \beta_m^{(1)}, \beta_m^{(2)})$ is given by Eq. (7.9). f has the form (7.5) but with $\alpha_m^{(3)}$, $\beta_m^{(3)}$ instead of $\alpha_m^{(1)}$, $\beta_m^{(1)}$, respectively.

The two spin correlation functions on the same time row have the form

$$\left\langle \exp\left[\frac{2\pi i}{q} m(l_r - l_0)\right]\right\rangle = a_m\left(\frac{\lambda_m}{\lambda_0}\right)^r \tag{7.12}$$

where

$$\lambda_m = \sum_{\rho=0}^{q-1} h_\rho \exp\left(\frac{2\pi i}{q} m\rho\right) \tag{7.13}$$

and $\{a_m\}$ are coupling-independent constants.

The generalization of these results to include external fields is straightforward. The calculations are more difficult and the results less transparent, though.

8. CONSTRUCTING RANDOM, STOCHASTIC CRYSTALS: EXACT SOLUTION OF A CONSTRAINED SPIN GLASS MODEL

In this section the method of constructing Monte Carlo (stochastic) crystals is generalized into a different direction. Let us consider again a

type of Ansatz as shown in Fig. 1. As discussed in Section 2, the Ansatz problem itself is defined as a one-dimensional Ising (or Potts, . . . etc.) problem, or alternately, as a Markov process given through the matrix (2.4). The Ansatz problem can be generalized to include random bonds:

$$-\frac{E^A}{k_B T} = \sum_j (\alpha_j s_{2j} s_{2j+1} + \beta_j s_{2j-1} s_{2j}) \tag{8.1}$$

where α_j (β_j) is a random variable sampled from the distribution $P(\alpha)$ [$R(\beta)$]. The free energy corresponding to (8.1)—and not to the Monte Carlo crystal—is calculated as

$$f = \frac{\ln Z_N}{N} = \frac{1}{N} \sum_{j=1}^{N/2} \ln 4 \cosh \alpha_j \cosh \beta_j$$

$$\xrightarrow[N\to\infty]{} \ln 2 + \frac{1}{2} \int d\alpha\, P(\alpha) \ln \cosh \alpha + \frac{1}{2} \int d\beta\, R(\beta) \ln \cosh \beta \tag{8.2}$$

The correlation function between two spins at a distance $r = 2k$ apart can be calculated as

$$\frac{1}{N} \sum_j \langle s_j s_{j+2k} \rangle = \frac{1}{N} \sum_j \prod_{i=j}^{k} (\tanh \alpha_i \tanh \beta_{i+1})$$

$$\xrightarrow[N\to\infty]{} \left[\int d\alpha\, P(\alpha) \int d\beta\, R(\beta) (\tanh \alpha \tanh \beta) \right]^k \tag{8.3}$$

Similarly, all correlations between even-numbered spins are exactly the same as the corresponding correlations between odd-numbered spins. Therefore, the probability distribution of the even-numbered and of the odd-numbered spins should also be identical. This proves that the construction described in Section 2 leads to an equilibrium triangular crystal. In this particular case the disorder constraint is a local condition. Every horizontal bond $K_3(i)$ in every up-pointing triangle (i) must satisfy the condition

$$K_3(i) = \tfrac{1}{2} \ln \{ \cosh [K_1(i) + K_2(i)] / \cosh [K_1(i) - K_2(i)] \} \tag{8.4}$$

where (i) is now an index numbering the up-pointing triangles and $K_1(i)$, $K_2(i)$ are random variables distributed according to $P(K_1)$ and $R(K_2)$, respectively. Note that Eq. (8.4) implies

$$\operatorname{sgn} [K_1(i) K_2(i) K_3(i)] = -1 \tag{8.5}$$

expressing the competition between spins. In general Eq. (8.4) does not imply, however, a full frustration[30] of the elementary triangles. The free energy per spin of the equilibrium crystal is given by

$$f(\beta) = \ln 2 + \frac{1}{2} \int \int dK_1\, dK_2\, P(K_1) R(K_2) [A + \ln \cosh K_3] \tag{8.6}$$

where

$$A(K_1, K_2) = \tfrac{1}{2}\ln\left[\cosh(K_1 + K_2)\cosh(K_1 - K_2)\right] \tag{8.7}$$

The results presented here can be extended to the case when the external field is not zero. In that case the Ansatz transfer matrices do not commute and even the solution of the Ansatz problem becomes quite sophisticated.[31] The situation is more simple if one deals with Ansatze whose transfer matrices commute, as for the general $Z(q)$ models discussed in the previous section.

We find the presence of disorder subspaces in random systems with competing interactions quite remarkable. One may guess that the disorder subspaces should play an even more important role in spin glasses than in nonrandom models. Further work is needed to fully exploit the physics contained in these solutions.

9. CONCLUSIONS

In this paper a large body of exact results had been obtained using a method akin to the methods previously used in parts I and II. Again, this method is inherently related to a dynamic process: here it corresponds to a

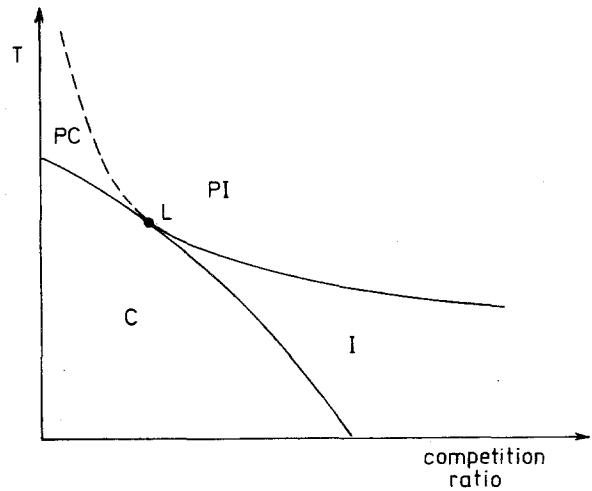

Fig. 11. The structure of the phase diagram near a Lifshitz point (L). PC denotes a paramagnetic phase with a monotonic decay of correlations, PI a paramagnetic phase with a modulated decay, C an ordered (commensurate) phase, and I a helical (floating or incommensurate) phase. Note the disorder line (dotted line) ending on the Lifshitz point.

stochastic model of crystal growth. Besides reconsidering the eight-vertex model, disorder subspaces had been calculated for the staggered eight-vertex model, the general (staggered) IRF model, for the triangular Potts model with fields, a general $Z(q)$ model including chiral terms, and, finally, for spin glass models. This wide range of applicability is not restricted to two-dimensional models. An example of a three-dimensional model with $d = 2$ Ising-type phase transition had been already presented in I.

As far as the physical implications of these results are concerned, it seems that further applications are possible—besides the calculation of multicritical points, the monitoring of changes in the pattern of correlations, etc. (see I). A recent example relates the disorder solution (2.12)[6] to the problem of directed animals.[4] Another example is the following. On physical grounds it is quite plausible that a Lifshitz point (a multicritical point on the common border of a disordered, an ordered–commensurate, and a helical–incommensurate–phase) should have the "fine" structure shown in Fig. 11, that is, there is a disorder line ending on L. The absence of such a disorder line in the chiral clock models[28] can be considered as an indication that—as recently shown[32]—the floating phase extends up to the decoupling point for $q = 3, 4$.

Finally, the presence of disorder lines in fully frustrated and random spin systems indicates that—at least at low temperatures—the modulated paramagnetic phase may be interpreted as a precursor of the fully developed spin glass phase. Indeed, Monte Carlo simulations[33] of nonrandom models with competing interactions suffer from the same lack of ergodicity as the spin glass models.[34]

ACKNOWLEDGMENTS

I am grateful to Professor I. Peschel for critical correspondence and for correcting some misprints in paper II. I am indebted to Professor R. J. Baxter for calling my attention to the work of Enting.[5] As may be already obvious to the reader, that line of thought made the calculations of this paper feasible.

APPENDIX A: FREE ENERGY AND CORRELATION FUNCTIONS OF THE EIGHT-VERTEX MODEL ON THE DISORDER SUBSPACE

Consider the Ansatz problem shown in Fig. 4a. By integrating spin-by-spin it is easy to see that the transfer matrix eigenvalue problem has the

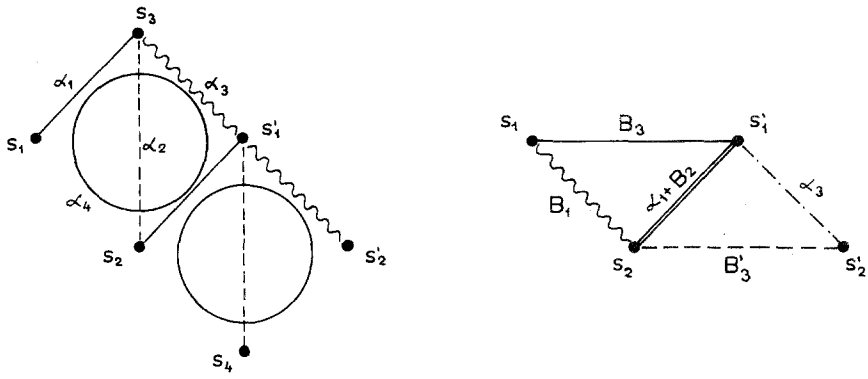

Fig. 12. Graphical representation of the transfer matrix for the calculation of free energy and correlations in the eight-vertex model.

following form (in the notation of Fig. 12):

$$\sum_{s_1,s_2}\sum_{s_3,s_4}\exp\{\alpha_1(s_1s_3+s_2s_1')+\alpha_2(s_2s_3+s_1's_4)+\alpha_3(s_3s_1'+s_1's_2')$$
$$+\alpha_4(s_1s_3s_2s_1'+s_1's_2's_4s_2)\}\Psi(s_1,s_2)=\tilde{\lambda}\Psi(s_1',s_2') \qquad (A.1)$$

It is useful to sum up first the spins s_3 and s_4 using Eqs. (3.1)–(3.2). One obtains then the simpler equation

$$\sum_{s_1,s_2}\exp\{B_1s_1s_2+\alpha_3s_1's_2'+B_3s_1s_1'+B_3's_2s_2'+(\alpha_1+B_2)s_1's_2\}\Psi(s_1,s_2)$$
$$=\lambda\Psi(s_1',s_2') \qquad (A.2)$$

where A, B_1, B_2, and B_3 are given in Eq. (3.2), while A', B_1', etc. are the same functions but for $\alpha_1=\alpha_3=0$. Also

$$\lambda=e^{A+A'}\tilde{\lambda} \qquad (A.3)$$

The 4×4 matrix defined by (A.2) can be further reduced to two 2×2 blocks corresponding to even and odd eigenvectors, respectively. The even (odd) subspace is

$$\begin{bmatrix} 2e^{2(\alpha_3+B_1)}\dfrac{\cosh}{\sinh}(\alpha_1+B_2+B_3+B_3'); & 2e^{B_1-\alpha_3}\dfrac{\cosh}{\sinh}(\alpha_1+B_2+B_3-B_3') \\ 2e^{\alpha_3-B_1}\dfrac{\cosh}{\sinh}(B_3-B_3'-\alpha_1-B_2); & 2e^{-2(\alpha_3+B_1)}\dfrac{\cosh}{\sinh}(B_3+B_3'-\alpha_1-B_2) \end{bmatrix} \qquad (A.4)$$

The eigenvalues of the even subspace are given by

$$\lambda_{1,2} = a^{(+)} + d^{(+)} \pm \left[\left(a^{(+)} - d^{(+)}\right)^2 + 4b^{(+)}c^{(+)} \right]^{1/2} \tag{A.5}$$

where

$$\begin{aligned} a^{(\pm)} &= e^{2(\alpha_3 + B_1)} \frac{\cosh}{\sinh}(\alpha_1 + B_2 + B_3'), \\ b^{(\pm)} &= e^{B_1 - \alpha_3} \frac{\cosh}{\sinh}(\alpha_1 + B_2 + B_3 - B_3') \\ c^{(\pm)} &= e^{\alpha_3 - B_1} \frac{\cosh}{\sinh}(B_3 - B_3' - \alpha_1 - B_2), \\ d^{(\pm)} &= e^{-2(\alpha_3 + B_1)} \frac{\cosh}{\sinh}(B_3 + B_3' - \alpha_1 - B_2) \end{aligned} \tag{A.6}$$

For the odd subspace one has

$$\lambda_{3,4} = a^{(-)} + d^{(-)} \pm \left[\left(a^{(-)} - d^{(-)}\right)^2 + 4b^{(-)}c^{(-)} \right]^{1/2} \tag{A.7}$$

The free energy per spin of the model (3.3) is given through λ_1 after the changes $B_1 \to -B_1$, $B_2 \to -B_2$; $B_3 \to -B_3$ are made:

$$f = \tfrac{1}{4} \ln \lambda_1 = \tfrac{1}{4} \ln \tilde{\lambda}_1 + \tfrac{1}{4}(A + A') \tag{A.8}$$

with

$$A' = \tfrac{1}{2} \ln 2^2 \cosh(\alpha_2 + \alpha_4) \cosh(\alpha_2 - \alpha_4) \tag{A.9}$$

instead of the (A.6) values.

The correlation functions of spins on the same horizontal (time) row are given by

$$\langle s_0 s_r \rangle = A_3 \left(\frac{\lambda_3}{\lambda_1} \right)^r + A_4 \left(\frac{\lambda_4}{\lambda_1} \right)^r \tag{A.10}$$

where

$$A_\alpha = \sum_{s_1, s_2} \Psi_1^{\text{left}}(s_1, s_2) s_1 \Psi_\alpha^{\text{right}}(s_1, s_2) \Psi_\alpha^{\text{left}}(s_1', s_2') s_1' \Psi_1^{\text{right}}(s_1', s_2') \tag{A.11}$$

$\Psi_\alpha^{\text{left(right)}}(s_1', s_2')$ is the left (right) eigenvector corresponding to the eigenvalue λ_α, $\alpha = 1, \ldots, 4$. All possible correlations between the Ansatz spins shown in Fig. 4a may be calculated in a similar way using the spectral decomposition of the kernel (A.1). Note that if $B_2 = -\alpha_1$ the matrix can be symmetrized and λ_3 and λ_4 are always real. However, in general, it is possible to change λ_3, λ_4 from real to a complex conjugate pair by varying the Ansatz parameters. In the latter case

$$\langle s_0 s_r \rangle = 2A \left(\frac{\lambda^{\text{odd}}}{\lambda_1} \right)^r \cos(qr + \varphi) \tag{A.12}$$

where $\lambda_{3,4} = \lambda^{\text{odd}} e^{\pm iq}$; $A_{3,4} = Ae^{\pm i\varphi}$. λ^{odd}, q, A, and φ are real functions of α's. The limiting case where the monotonic decay(s) (A.10) changes into a modulated decay (A.12) is given by $\lambda_3 = \lambda_4$ or

$$\left[a^{(-)} - d^{(-)}\right]^2 + 4b^{(-)}c^{(-)} = 0 \tag{A.13}$$

with $a^{(-)}, b^{(-)}, c^{(-)}$ given in Eq. (A.6). Then in Eq. (A.12) $q = \varphi = 0$ and one encounters a single exponential decay. This corresponds to the cases treated in II.

APPENDIX B: FREE ENERGY AND CORRELATION FUNCTIONS OF THE TRIANGULAR POTTS MODEL ON THE DISORDER SUBSPACE

The Ansatz problem is given by Eq. (6.1). First, let us remember that the three-spin interaction is not translational invariant, but contains only the odd-numbered spins and their NN neighbors. This results in a difference of the correlation functions on $t = 2k\Delta t$ and $t = (2k + 1)\Delta t$ layers. For the sake of simplicity we consider here only the case $\gamma = 0$, when this problem does not occur. As shown in Appendix A, it is useful to perform first an iteration transformation by summing up every second spin. The Ansatz partition function transforms as

$$Z_N^{\text{Ansatz}}(\alpha_1, \alpha_2, \beta_0, \beta_1, \beta_2) = e^{NA/2} \tilde{Z}_{N/2}^{\text{Ansatz}}(B, C_1, C_2, D) \tag{B.1}$$

where A, B, C_1, C_2, and D are functions of $\alpha_1, \alpha_2, \beta_0, \beta_1, \beta_2$ as given in Eqs. (6.3) ($\gamma = 0$). The remaining spins form now a uniform Potts chain with interactions given by Eq. (6.2). The corresponding one-dimensional transfer matrix has the form

$$\mathrm{t} = \begin{bmatrix} e^{B+D+C} & e^{C/2} & e^{C/2} & \cdots \\ e^{C/2} & e^{B} & 1 & \cdots \\ e^{C/2} & 1 & e^{B} & \cdots \\ \vdots & \vdots & \vdots & \end{bmatrix} \tag{B.2}$$

where $C = C_1 + C_2 + \beta_0$. The eigenvalues and eigenvectors of this matrix are easily computed. The eigenvalues are

$$\begin{aligned} \lambda_{1,2} &= \tfrac{1}{2}\Big\{ e^{B+D+C} + e^{B} + q - 2 \\ &\qquad \pm \left[\left(e^{B+D+C} - e^{B} - q + 2\right)^2 + 4e^{C}(q-1) \right]^{1/2} \Big\} \\ \lambda_{3,\ldots,q} &= e^{B} - 1 \end{aligned} \tag{B.3}$$

The free energy per spin of the Potts model (6.4) is accordingly given by

$$f = \tfrac{1}{2}A + \tfrac{1}{2}\ln\tilde{\lambda}_1 \tag{B.4}$$

where

$$\tilde{\lambda}_1 = \lambda_1(B \to K_3\,; C \to H; D \to M_3) \tag{B.5}$$

In order to calculate the correlation functions we need also the eigenvectors of the matrix (B.2). They have the following form:

$$|\alpha\rangle = \begin{bmatrix} 1 \\ x_{1,2} \\ x_{1,2} \\ \vdots \\ x_{1,2} \end{bmatrix}, \qquad \alpha = 1, 2,$$

$$|\alpha\rangle = \begin{bmatrix} 0 \\ \rho^{(\alpha-2)} \\ \vdots \\ \rho^{(q-2)(\alpha-2)} \end{bmatrix}, \qquad \alpha = 3, \ldots, q, \quad \rho = e^{2\pi i/(q-1)} \tag{B.6}$$

Consider the correlation functions of the form

$$\langle e^{(2\pi i/q)m(l_0 - l_r)} \rangle = \sum_{\alpha=1}^{q} \left(\frac{\lambda_\alpha}{\lambda_1} \right)^r |\langle 1|\hat{\sigma}_3^m|\alpha\rangle|^2 \tag{B.7}$$

where l_0, l_r are Potts variables on the same time row (t = const) and $\hat{\sigma}_3$ is a diagonal matrix

$$\hat{\sigma}_3 = \begin{bmatrix} 1 & & & & \\ & \omega & & & \\ & & \omega^2 & & \\ & & & \ddots & \\ & & & & \omega^{q-1} \end{bmatrix}, \qquad \omega = e^{2\pi i/q} \tag{B.8}$$

Thus the correlation functions (B.7) consist of a constant term corresponding to the square of the "magnetization" and $(q-1)$ terms decaying exponentially—since the matrix (B.2) is symmetric, all eigenvalues are real.

REFERENCES

1. P. Ruján, *J. Stat. Phys.* **29**:231 (1982).
2. I. Peschel and V. J. Emery, *Z. Phys. B* **43**:241 (1981).
3. P. Ruján, *J. Stat. Phys.* **29**:247 (1982).
4. D. Dhar, *Phys. Rev. Lett.* **49**:959 (1982); *Phys. Rev. Lett.* **51**:853 (1983).

5. I. G. Enting, *J. Phys. C* **10**:1379, 1023 (1977); **11**:555, 2001 (1978).
6. A. M. Verhagen, *J. Stat. Phys.* **15**:219 (1976).
7. T. R. Welberry and R. Galbraith, *J. Appl. Crystallogr.* **6**:87 (1973); **8**:636 (1975).
8. B. M. McCoy and T. T. Wu, *Phys. Rev.* **176**:631 (1968).
9. Yu. G. Stroganov, *Phys. Lett. A* **74**:116 (1979); R. J. Baxter, *J. Stat. Phys.* **28**:1 (1982).
10. K. Binder, in *Phase Transitions and Critical Phenomena*, Vol. V, C. Domb and M. S. Green, eds. (Academic Press, New York, 1976).
11. O. Perron, *Math. Ann.* **64**:248 (1907); S. B. Frobenius, *Pressus. Acad. Wiss.* 471 (1908).
12. J. Dóczi-Réger and P. C. Hemmer, *Physica A* **108**, 531 (1981).
13. G. H. Wannier, *Rev. Mod. Phys.* **17**:50 (1945); I. Syozi in *Phase Transitions and Critical Phenomena*, Vol. I, C. Domb and M. S. Green, eds. (Academic Press, New York, 1972).
14. J. Stephenson, *Phys. Rev. B* **1**:4405 (1970); *J. Math. Phys.* **5**:1009 (1964); **7**:1123 (1966); **11**:413, 420 (1970).
15. R. J. Baxter, *Exactly Solved Models in Statistical Mechanics* (Academic Press, London, 1982).
16. I. Peschel and F. Rys, *Phys. Lett. A* **91**:187 (1982).
17. V. G. Vaks, A. I. Larkin, and Yu. N. Ovchinikov, *Zh. Eksp. Teor. Fiz.* **49**:1180 (1965) [*Sov. Phys. JETP* **22**:820 (1966)] and Ref. 14.
18. R. J. Elliott, *Phys. Rev.* **124**:346 (1961); W. Selke, *Z. Phys. B* **29**:133 (1978); M. E. Fisher and W. Selke, *Phys. Rev. Lett.* **44**:1502 (1980); *Phys. Rev. B* **20**:257 (1979); P. Bak and F. van Boehm, *Ibid.* **21**:5297 (1980); S. Redner and H. E. Stanley, *Ibid.* **16**:4901 (1977).
19. P. Rujan, *Phys. Rev. B* **24**:6620 (1981).
20. J. Ashkin and E. Teller, *Phys. Rev.* **64**:178 (1943).
21. F. J. Wegner, *J. Phys. C* **5**:L131 (1972); F. Y. Wu, *J. Math. Phys.* **18**:611 (1977).
22. For a review see E. H. Lieb and F. Y. Wu, in *Phase Transitions and Critical Phenomena*, Vol. I, C. Domb and M. S. Green, eds. (Academic Press, New York, 1972).
23. R. B. Potts, *Proc. Camb. Phil. Soc.* **48**:106 (1952).
24. For a review and further references see F. Y. Wu, *Rev. Mod. Phys.* **54**:235 (1982).
25. W. F. Wolff and J. Zittartz, *Z. Phys. B* **50**:131 (1983) and references therein.
26. A. N. Berker and L. P. Kadanoff, *J. Phys. A* **13**:L259 (1980).
27. D. A. Huse, *Phys. Rev. B* **24**:5180 (1981).
28. S. Ostlund, *Phys. Rev. B* **24**:398 (1981).
29. S. Elitzur, R. B. Pearson, and J. Shigemitsu, *Phys. Rev. D* **19**:3698 (1979).
30. G. Toulouse, *Commun. Phys.* **2**:115 (1977).
31. C. Fan and B. M. McCoy, *Phys. Rev.* **182**:614 (1969).
32. F. Haldane, P. Bak, and T. Bohr, *Phys. Rev. B* **28**:2743 (1983); H. J. Schulz, *Phys. Rev. B* **28**:2746 (1983).
33. W. Selke and M. E. Fisher, *Z. Phys. B* **40**:71 (1980); W. Selke, *Ibid.* **43**:335 (1981); I. Morgenstern, *Phys. Rev. B* **26**:5296 (1982).
34. For a review see K. Binder, in *Ordering in Strongly Fluctuating Condensed Matter Systems*, T. Riste, ed. (Plenum, New York, 1980).